International Symposium of Research Students on Materials and Engineering
December 20-22, 2004, Chennai, India
Department of Metallurgy and Materials Engineering, Indian Institute of Technology Madras

CREEP DEFORMATION BEHAVIOUR OF TITANIUM MODIFIED AUSTENITIC STAINLESS STEEL

S.Latha, M.D.Mathew, K.Bhanu Sankara Rao and S.L.Mannan
Metallurgy and Materials Group, Indira Gandhi Centre for Atomic Research
Kalpakkam, India

ABSTRACT

Titanium modified austenitic stainless steel also called alloy D9, is the current choice of material for fuel cladding and wrapper material for fast reactors. The creep properties of this steel have been evaluated in the 20% cold worked condition at 923 K at various stress levels on tubular specimens. The results have been compared with type 316 stainless steel (316 SS) clad tubes. Alloy D9 clad tubes exhibited better creep strength than type 316 stainless steel clad tubes. The apparent activation energy for creep deformation of alloy D9 clad tubes was estimated to be around 450 kJ/mol. Creep ductility of alloy D9 tubes was very low when compared to 316 stainless steel clad tubes.

Key words: Alloy D9, 316 SS clad tube, activation energy

1.0 INTRODUCTION

15Cr-15 Ni –2.2 Mo-Ti modified stainless steel, similar to the alloy specified in ASTM A771-88 (UNS 38660) also known as alloy D9 has been chosen for fuel clad and fuel subassembly wrapper material for the Proto type Fast Breeder Reactor (PFBR) which is being constructed at Kalpakkam. The core of the Fast Breeder Reactor (FBR) consists of a large number of subassemblies containing the fuel pins. FBR fuel subassemblies are expected to withstand severe operating conditions of sodium environment and elevated temperatures. High temperature service would result in degradation in mechanical properties. Moreover clad and wrapper materials should possess resistance to radiation induced dimensional changes, void swelling and irradiation creep. Hence alloy D9 is developed by adjusting the composition of 316 SS, from considerations of radiation damage viz, lower void swelling and irradiation creep, which limits the burn up (amount of fissile material consumed) of the fuel of fast reactors. Minor elements like titanium, silicon and phosphorus are found to be effective in increasing the swelling resistance of austenitic stainless steels. Alloy D9 contains additions of titanium, higher level of nickel and lower level of chromium than 316 SS[1]. As cold-work plays an important role in reducing irradiation induced void swelling of stainless steels, alloy D9 would be used with an optimum cold work of 20% in fast reactors[2].

In PFBR, the fuel clad tubes experience temperatures in the range of 673-973 K under steady state operating conditions. Under steady operating conditions of the reactor, the clad tubes would be subject to a temperature profile that increases from 673K at lower ends to 973K at the top of the fuel subassemblies. Under transient conditions, the temperatures can rise upto1273 K[3]. Thermal creep resistance of the fuel tubes is therefore an important consideration in the design of fuel subassemblies. The thermal creep properties of alloy D9 are evaluated at 923 K and compared with those of 316 SS clad tubes. This paper deals with the thermal creep

behaviour of 20% cold-worked alloy D9 cladding tubes at 923 K. The creep properties of alloy D9 are compared with the data obtained on 316 SS clad tubes.

2.0 EXPERIMENTAL

20% cold worked alloy D9 tubes were procured from M/s. Valinox France. Type 316 stainless steel tubes in 20% cold worked condition were procured from M/s. Fine tubes, UK. The chemical compositions of D9 tubes and 316 SS tubes are given in table 1.

Creep tests were performed at 923 K at stress levels of 175, 200, 225,250 and 300 MPa. Creep tests were also conducted to evaluate the activation energy for alloy D9 clad tubes in the stress levels of 125,175 and 225 MPa. These tests were initially started at 923 K and the temperature was raised in steps of 25 K after the creep rate attained a minimum value at that particular temperature. Alloy D9 tubes had a nominal dimension of 6.60 mm outside diameter and 0.45 mm wall thickness. The outside diameter of 316 stainless steel cladding tubes was 5.10 mm and the wall thickness was 0.37 mm. Tubular creep specimens were made by welding tubes of 100 mm length to mandrels (end plugs) at both the ends. The effective gauge length of the specimen was 50 mm. Constant load creep tests were carried out by using SATEC single lever creep machines. The test temperature was controlled within ±2K during the tests. Creep elongation was measured using linear variable differential transducers. Optical and scanning electron microscopic investigations were carried out to examine the microstructure and fracture behaviour respectively.

3.0 RESULTS AND DISCUSSION

Figure 1. shows the variation of creep strain rate with creep strain for alloy D9 and 316 SS at 200 MPa. The creep strain rate decreases with increase in strain, it reaches a minimum value and then it increases again. Alloy D9 clad tubes crept at a much lower rate than 316 SS tubes. The addition of titanium substantially lowers the creep rate and increases the strength.

It is generally assumed that the minimum creep rate $\dot{\varepsilon}$ dependence on stress σ and temperature T can be expressed by the equation

$$\dot{\varepsilon} = A\sigma^{n}\exp(-Q/RT)$$

where A is a material constant, n is the stress exponent, Q is the apparent activation energy and R is the gas constant.

The values of minimum creep rate obtained for alloy D9 and 316 SS are plotted as a function of applied stress in Fig.2. The value of stress exponent was around 12 for 316 SS clad tubes and around 11 for alloy D9 clad tubes. The stress exponent values obtained are indicative of dislocation creep. In austenitic stainless steel, elevated temperature exposure during creep leads to precipitation of carbides on grain boundaries and on matrix dislocations. The stress dependence of creep rate in such cases is determined primarily by the stress dependence of the mobile dislocation link density, which is a function of the dislocation link lengths. Precipitation of fine carbides on the dislocations leads to small interparticle spacing and hence short link lengths. The smaller the link length, higher is the link density and thus higher is the creep stress exponent[4,5] .

Creep deformation mechanisms are identified in terms of the stress exponent n and the activation energy Q. Generally, in pure metals and solid solutions, values of n=3 to 5 have been associated with dislocation creep, while diffusion creep is characterised by n=1, and grain

boundary sliding controlled creep is identified with value of n=2. In precipitation hardened and dispersion strengthened materials, much higher values of n (as high as 40) have been reported[6]. In austenitic stainless steels, precipitation usually takes place during creep and values of` n intermediate between those of solid solution alloys and precipitation hardened/ dispersion strengthened materials have been generally reported[4,5].

The activation energy for creep was determined from temperature change creep tests carried out at 125,175 and 225 MPa. Initially the test was started at 923K and the temperature was increased in steps of 25 K, till fracture (~1073 K) after a minimum value of creep rate was attained at that temperature. Plot of minimum creep rate with reciprocal of temperature for all the stress levels is shown in Fig.3. Since the temperature change tests were carried out at a constant load (constant nominal stress), the normalised stress (stress normalised with Young's modulus at that temperature) at the highest test temperature (1073) K was about 8% higher than its value at the lowest test temperature (923 K).

The apparent activation energy energy values obtained were 430,446, and 472 kJ/mol for 125,175 and 225 MPa respectively and the average was around 450 kJ/mol. As there were no significant changes in activation energy values with increase in stress, there is no change in creep mechanism in the range of stress investigated. The activation energy value obtained is much higher than the activation energy for self diffusion of iron. Similar values of activation energy were obtained for type 321 stainless steels by Snowden et al[7],Bernard et al[8] for 316 stainless steel and for 20Cr-25 Ni austenitic stainless steel by Yamane et al[9] and for 347 stainless steel[10].

The higher value of activation energy obtained may be attributed to precipitation of titanium carbide which produces back stress and hence more activation energy, for creep deformation. Creep behaviour can be explained by a recovery model modified with respect to second phase particles[11]. The creep rate can be expressed by

$$\dot{\varepsilon} = A(\sigma - \sigma_0)^{n_0} \exp(-Q)/RT$$

where Q is the activation energy for creep, $(\sigma - \sigma_0)$ is the effective stress on mobile dislocations and the stress exponent n_0 is generally taken as 4. The back stress σ_0 produced by the particles accounts for the high value of n calculated in materials hardened by a second phase as well as the discrepancy between self diffusion and creep activation energies. In order to determine the back stress, a plot of (minimum creep rate)$^{1/4}$ vs. applied stress was made (Fig. 4) and the extension of this line to creep rate equal to zero on the stress axis gives the value of back stress. The value of back stress was estimated to be around 143 MPa. Figure 5 shows the variation of minimum creep rate with effective stress $(\sigma - \sigma_0)$. The stress exponent value $n_0$was determined to be around four.

The variation of rupture life with applied stress for these materials is shown in Fig.6. Creep strength of alloy D9 is greater than 316 SS by a factor of four. A power law relationship was found to exist between applied stress, σ and rupture life, t_r for both alloy D9 and 316 SS. The improvement in strength can be attributed to the presence of titanium carbide in the alloy. The stability of microstructure against recovery and recrystallisation by fine TiC precipitates gives higher strength to the alloy. Presence of titanium carbide (TiC) and $M_{23}C_6$ precipitates were confirmed by using X ray diffraction in this alloy after testing at 175 MPa.

Fujiwara et al [12] have studied the creep properties of 20% cold worked 316 stainless with additions of titanium (Ti content 0- 1.09 wt%). The titanium to carbon ratios (Ti/C) were varied between 0.5 and 15. They observed that 1000h creep rupture strength showed a peak at titanium content between 0.22 and 0.32 wt%, corresponding to Ti/C ratio between three and five. The

improvement in strength by titanium additions upto 0.3 wt% can be attributed to the increase in finely dispersed TiC precipitates instead chromium carbides, $M_{23}C_6$ in the matrix. In type 316 SS coarsening of carbides take place enabling recovery and thus decreasing the efficiency of precipitation strengthening. On the other hand, in alloy D9, the carbide particles will be finer in size than in 316 SS, thereby giving rise to higher creep rupture strength[13]. Kesternich and Meertens[14] have systematically studied the influence of thermomechanical treatments on the evolution of microstructure in a similar steel (DIN 1.4970).

It was found that a fine dispersion of TiC precipitates strongly retarded the recovery and recrystallisation of cold worked material by pinning dislocations and grain boundaries. Vasudevan et al[15] have investigated the influence of thermomechanical treatments on alloy D9 and they observed an optimum level of 20% cold work retards the recovery and recrystallisation by TiC precipitates.

A power law relationship, $t_t=At_r^{\beta}$ (where t_t is the time to onset of tertiary, A and β are constants, t_r is the rupture life) was found to be obeyed between the time to onset of tertiary and rupture life. The time to onset of tertiary is plotted against rupture life in Fig. 7. The equation for alloy D9 is $t_t=0.63t_r^{0.98}$ and for 316 is $t_t = 0.13t_r^{1.2}$ As the exponent β was around 1 for both alloy D9 and 316 SS, then A is approximately equal to t_t/t_r. Hence it can be concluded that the time spent before the onset of tertiary creep as a function of time to rupture is more for alloy D9 than 316 SS.

The variation of rupture elongation with rupture life is shown in Fig.8. Rupture ductility for alloy D9 tubes did not exhibit much variation with rupture life.

In 316 clad tubes the rupture ductility was found to decrease with increase in rupture life. This is due to coarsening of $M_{23}C_6$ carbides and intermetallic phases in stainless steel. Rupture ductility of alloy D9 was rather low (<10%).

Microstructural studies on creep tested alloy D9 indicated the occurrence of numerous grain boundary triple cracks in the grain boundaries (Fig.9 (a)).

Scanning electron microscopic investigations revealed that the fracture mode was intergranular (Fig.9 (b)). The cold worked matrix coupled with precipitation of titanium carbides on the intragranular regions the matrix restricts matrix deformation and hence the low values in ductility.

CONCLUSIONS

A power law relationship was found to be obeyed between the applied stress and minimum creep rate. The power law for alloy D9 tube is

$$\dot{\varepsilon} = 2.63 \times 10^{-34} \sigma^{10.63} \exp(-450000/RT)$$

The higher activation energy values obtained can be attributed to the back stress provided by the precipitates. The back stress was estimated to be around 143 MPa. Rupture life of alloy D9 clad tubes was higher than those of type 316 SS clad tubes by a factor of about four. The enhanced life is attributed to the presence of titanium carbide precipitation in alloy D9. A power law relationship was found exist between the time to onset of tertiary and rupture life for both alloy D9 and 316 SS. Rupture elongation of alloy D9 tubes was very low less than 10%.

ACKNOWLEGEMENTS

The authors wish to thank Dr.Baldevraj, Director, Indira Gandhi Centre for Atomic Research, for his encouragement during the course of this work.

REFERENCES

1. Puigh R J and Hamilton M L , *Influence of Radiation on Material properties: 13th International symposium (part II),ASTM STP 956, Eds. Garner F A,* Henager C H jr and Igata N (1987), 22-29.
2. Brager H R, *Jour. Nucl Mater*, **57,** (1975, 103.
3. Latha S Mathew M D, Bhanu Sankara Rao K and Mannan S L, *Creep Properties of Alloy D9 Fuel Clad tubes for PFBR* (2004) IGC report No. 261.
4. Morris D G, and Harries D R, *Metal Sci* **12** , (1978), 525.
5. Mannan S L, and Rodriguez P, *Metal Sci*, **17** 1983, 63. 8.
6 Evans R W, and Wilshire B, *Introduction to Creep*, The Institute of Materials , (1993), 62.
7. Snowden K.U, Stathers P A., and Hughes D. S. , International conference on Strength of Metals and Alloys -ICSMA-6, (Eds) Gifkins **2,**Pergamon press,1983**.**
8. Bernard,L, Campo E, and Quaranta S *Mechanical Behaviour and Nuclear Applications of Stainless steels at Elevated Temperatures* ,The metals Society,1982,88.
9. Yamane Y, Takahashi T and Nakagawa K *Jour. Mater. Sci Letters*, **3**,(1984) 557.
10. Pilloni G, Quadrini E and Spigarelli S, *Mater.Sci & Engg*., **A279**, (2000),52.
11. Lagenbourg R, *Jour. Mater.Sci*,**3**, 1968, 596.
12. Fujiwara M, Uchida, H Yuhara S, tani S., and Satao Y., *Radiation induced changes in Microstructure; 13th ineternational Symposium (part I) ASTM STP 955*, Garner F A, Packan N H, and Kumar A S (eds.), *ASTM STP 955*, 127.
13. Kesternich W, Rothaut J, *Jour.Nucl. Mater*. **103&104** (1981) 845.
14. Kestrenich W and Meertens D *Acta Met*., (1986), **34**,161,1071.
15. Vasudevan M, Venkadesan S, and Siva Prasad P V, *Mater. Sci and Tech*, **12**, 1996, 338.

TABLES

Table 1
Chemical composition (wt%) of Alloy D9 ,316 SS clad tubes
and PFBR specifications for alloy D9.

Element	PFBR	Alloy D9	316 SS
C	.035-0.05	0.04	0.04
Ni	14.5-15.5	15.15	13.59
Cr	13.5-14.5	14.04	17.10
Mo	2.0-2.5	2.25	2.38
Ti	5C-7.5C	0.26	--
Si	0.5-0.75	0.61	0.33
Mn	1.65-2.35	1.78	1.88
S	0.01 max	<0.002	0.009
P	0.02 max	0.007	0.009
Al		0.006	0.005
B	10-20 ppm	0.0015	-
N	0.005 max	0.0037	0.044
Fe	balance	balance	balance

FIGURES

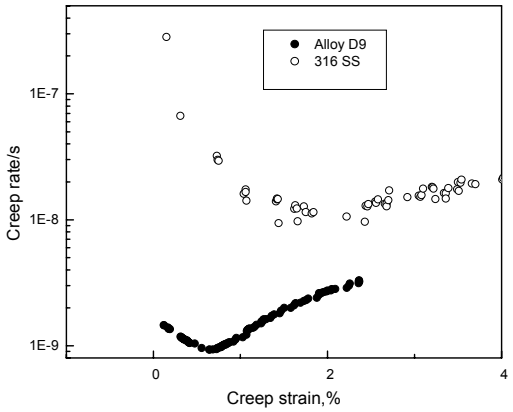

Fig.1. Creep rate vs. Creep strain for alloy D9 and 316 SS tubes

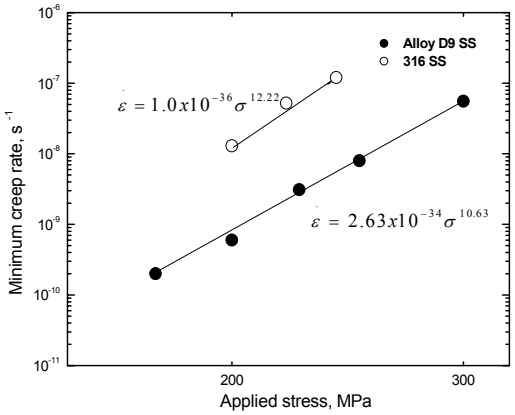

Fig.2. Power law creep at 923 K for 316 SS and D9 tubes.

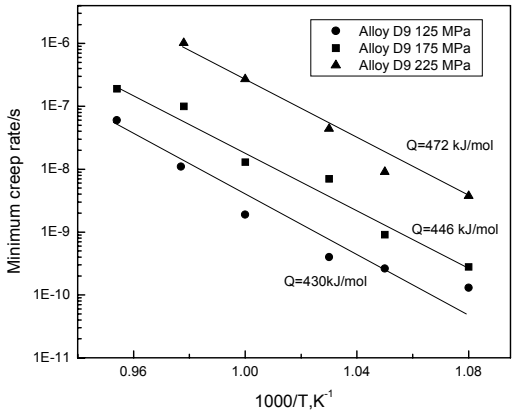

Fig.3. Arrhenius plots for Alloy D9

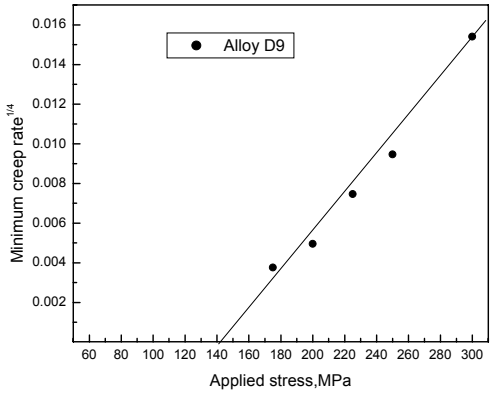

Fig.4. Plot of fourth root of minimum creep rate vs applied stress

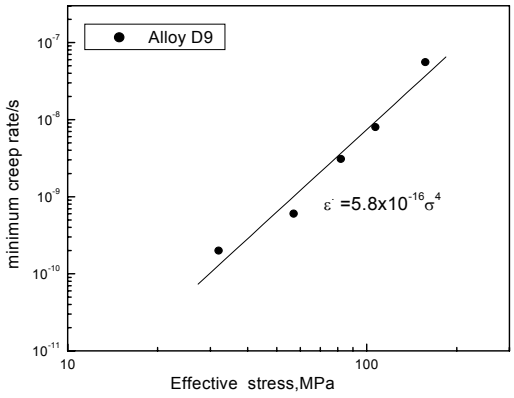

Fig.5. Effective stress vs. minimum creep rate

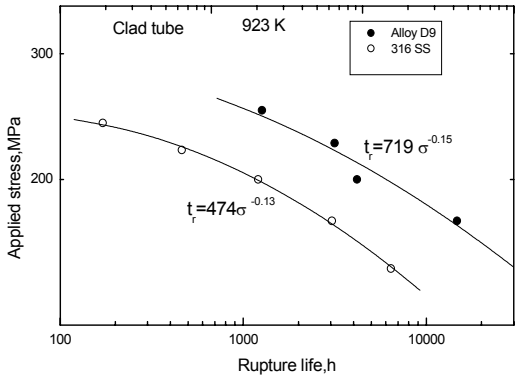

Fig.6. Creep strengths of alloy D9 and 316 SS tubes at 923 K.

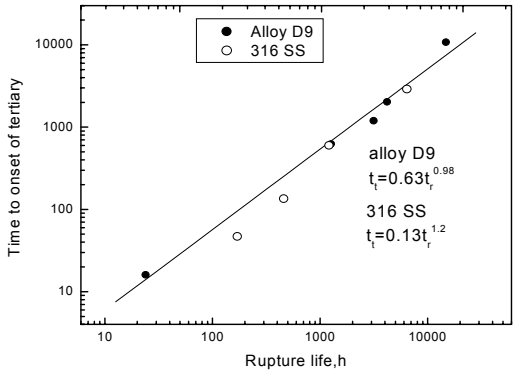

Fig.7. Relation between time to onset of tertiary and rupture life .

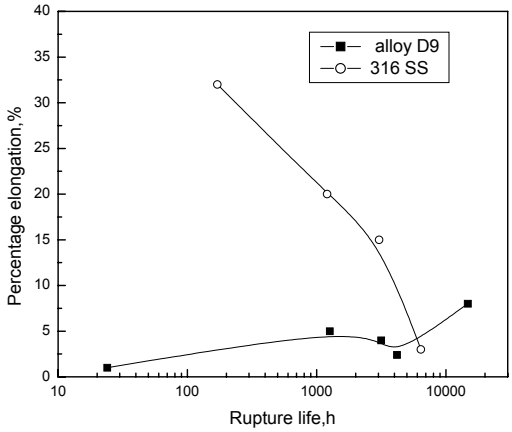

Fig.8.Comparison of ductilities of alloy D9 and 316 SS.

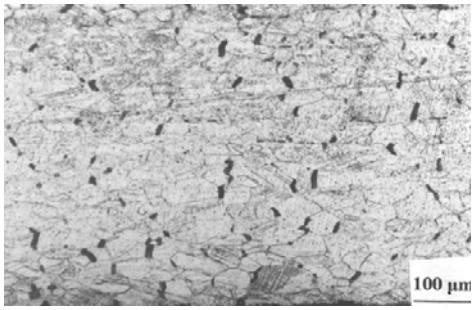

Figure 9(a). Wedge cracks in alloy D9 crept at 175 MPa

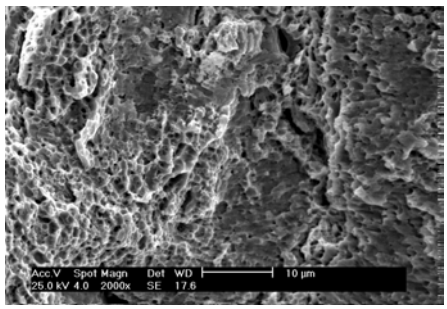

Fig.9(b). Fracture surface of alloy D9 crept at 250 Mpa